Possible origin of the crack pattern in deposition films formed from a drying colloidal suspension

Jun Ma[1,*] and Guangyin Jing[1,2,†]
[1]*Department of Physics, Northwest University*
[2]*NanoBiophotonics Center, National Key Laboratory and Incubation Base of Photoelectric Technology and Functional Materials, Xian 710069, China*

(Received 30 April 2012; revised manuscript received 22 August 2012; published 17 December 2012)

The fracture mechanics was usually employed to explain the crack propagation in the deposition produced by drying colloidal suspension. However, more complex than conventional fracture, those cracks periodically distribute and make up a unique pattern. Inspired by the concept of spinodal decomposition, here we develop the theory to illustrate the possible mechanism of the spatial arrangement of the cracks. It indicates that before the cracks develop and propagate in the deposition under the law of fracture mechanics, the periodically distributed flaws are generated by the phase separation of colloidal clusters and solvent. Then the cracks originate at the sites of those flaws in terms of fracture mechanics. It concludes that the crack spacing results from the wavelength of the concentration fluctuation during the phase separation, linearly growing with the increase of the deposition thickness and initial particle concentration, which is consistent with experimental results.

DOI: 10.1103/PhysRevE.86.061406 PACS number(s): 82.70.Dd, 82.70.Gg, 64.70.fm, 64.75.−g

I. INTRODUCTION

Colloidal depositions formed by drying suspension ubiquitously occur in both nature and technological application. Cracks widely exist in those depositions, which greatly limits and lowers their practical purposes. More elusive than ordinary cracks in routine materials, cracks in colloidal deposition periodically distribute and divide the two-dimensional (2D) deposit into uniform domains. These cracks separated by a distance make up the array pattern, which can be characterized by the wavelength (crack spacing) [1–5].

Crack patterns displayed versatile morphologies under various experimental conditions. With directional drying aqueous suspensions of silica, the pattern constituted by parallel cracks formed [6,7]. Okubo *et al.* demonstrated a spokelike crack pattern by drying a suspension of silica or polystyrene spheres [3,4]. A polygon pattern of cracks in the dried deposition was produced after evaporating starch slurry [1,5]. Shorlin *et al.* studied crack patterns formed by drying a thin layer of alumina-water slurry. The weblike crack pattern was generated from isotropic drying, whereas the parallel longitudinal pattern emerged on the condition of directional drying [2].

The fracture mechanics was employed to analyze the crack propagation [6–9]. Allain and Limat developed a model to suggest that the competition of the relaxation and increase of stress results in the regular crack spacing [7]. Tirumkudulu and Russel studied the cracks in the dried latex films, and found the scaling law of critical stresses derived from the concept of classical Griffith's energy balance [8]. The dynamics of crack propagation in silica gel was studied by linear elastic fracture mechanics. It was shown that the stress was released by the formation of cracks as it surpassed a threshold value [9]. Dufresne *et al.* worked on the dynamics fracture in dried silica films and discovered that the crack propagation was driven by the elastic energy, which was balanced by the energies of interface of crack and viscous dissipation of fluid [6].

On the other hand, first, the cracks periodically distribute, and make up the unique pattern. Second, the pattern depends on the deposition thickness [7,10] and particle concentration [4,11], etc. Inspired by the concept of spinodal decomposition [12], here we propose a theory to explore the origin of the pattern consisting of periodically parallel cracks.

II. COLLOIDAL CLUSTERS COALESCE IN THE DRYING PROCESS

Consider here that the colloidal suspension (hard spheres + distilled water) directionally dries on a rigid wettable plate (Fig. 1). Although the DLVO theory is valid for dilute suspensions, it can also be applied for higher solid contents on the condition of only main characteristic such as interaction energy being concerned [13]. Since the dilute suspension concentrates gradually in the whole evaporation process, the DLVO theory is adopted to describe the interaction energy between two colloidal particles (clusters) (see Appendix subsection A). The coalescence of colloidal particles results from the collision causing by Brownian motion. To simplify the analysis, we assume the doublet reaction to occur, which has been employed for the general analysis of colloidal aggregation [14]. Due to weak electrolyte environment (di-water), the repulsive electric force is strong so that particles coalesce by reaction-limited colloid aggregation (RLCA).

During the evaporation in the present case, the contact line of aqueous suspension is not pinned and continually retreats, laying the dried deposit (as indicated in Refs. [7,15]), which indicates that no flow replenishes solvent loss owing to the evaporation. The particle diffusion from inner suspension to the reaction area (drying front) can be neglected (Appendix subsection B). This is consistent with the Roth *et al.* experimental study of drying a colloidal droplet with a receding contact line, in which no particle transportation occurred by diffusion or flow from the inner drop to the drying front (near the contact line), where the particle deposit is generated from the concentrating due to the drying [15].

As indicated by the study of the interaction of colloid clusters, the shape of individual cluster can be approximately

*junma@nwu.edu.cn
†jing@nwu.edu.cn

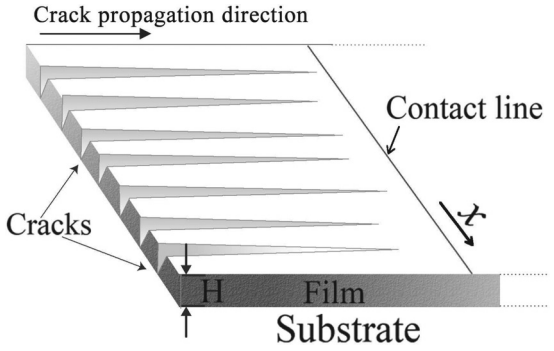

FIG. 1. Sketch of the crack pattern resulting from directional drying colloidal suspension on the rigid plate. Contact line is the receding line of the suspension during drying process.

treated as a sphere [16]. We consider that the clusters continuingly grow and separate each other with a distance ζ in the solvent. This physical configuration is confirmed by the x-ray scattering experiment for drying nanoparticle suspension [15,17]. After k coalescences (k doublet reactions), the number and radius of clusters in the suspension are

$$N = N_0/2^k, \tag{1}$$

$$R = 2^{k/3} r_0, \tag{2}$$

respectively, where N_0, r_0 are the initial number and radius of colloidal particles, respectively.

During the period for completing one coalescence, we can ignore the evaporation effect and consider that the number concentration is controlled by cluster coalescence. However, the evaporation effect on the concentration after relative long time has been achieved by shortening the distance of clusters ζ (Appendix subsection C).

III. PHASE SEPARATION OF COLLOIDAL CLUSTERS AND SOLVENT

At the late stage of the drying process, with water continuously evaporating, the air-liquid interface approaches just above the deposition, subsequently the air invades the upper layer of clusters to form a meniscus (Fig. 2). The capillary force results in water drainage from the clusters, leading to the coalescence of adjacent clusters. The change of surface energy in unit volume for the drainage of water from the clusters is

$$E = (\gamma_c - \gamma_{wc}) n 4\pi R^2 = 4\pi \gamma n R^2, \tag{3}$$

where n is the number of clusters in unit volume, γ_c and γ are the surface energy of cluster and water in air, respectively, γ_{wc} is the interfacial energy between water and cluster.

The maximum van der Waals potential of the coalescence of clusters is no more than $70KT \sim 2.8 \times 10^{-19}$ J at room temperature [13], which is far less than the driving energy here for phase separation of $\sim 3.1 \times 10^{-11}$ J, released from the surface energy ($2\gamma 4\pi R^2/6$, as one spherical cluster can coalesce with six neighboring spheres) for coalescing a pair of typical clusters of 10 μm diameter. Therefore, compared with the variation of surface energy in the process of phase separation, the van der Waals energy can be neglected.

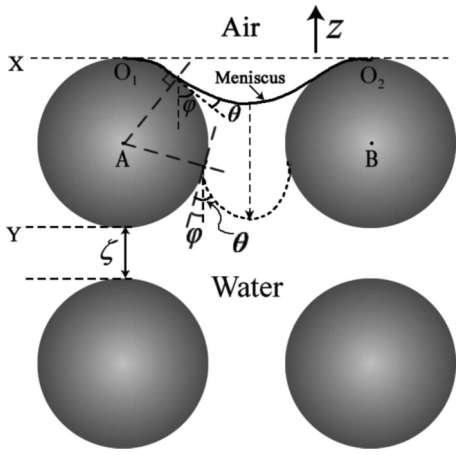

FIG. 2. Side view of the water drainage from the colloidal clusters. The dashed line O_1O_2 represents the air-water interface as the water drainage initiates. The meniscus forms as the air invades the clusters, and continually proceeds forward as indicated by the arrow.

The total work for water drainage in unit volume is (Appendix subsection D)

$$W = \tfrac{4}{3}\pi \gamma n R(2R + \zeta)\cos\theta, \tag{4}$$

where θ is the contact angle of water on the spherical cluster. To meet the energy criterion of water drainage $W - E \leqslant 0$, the surface distance of adjacent clusters satisfies

$$\zeta \leqslant R(3\sec\theta - 2). \tag{5}$$

During phase separating, water flow through the porous medium (clusters) is described by Darcy's law as [18]

$$Q = \frac{-kA}{\eta}\frac{\partial(\Delta P)}{\partial x}, \tag{6}$$

where Q is the flow rate, k is the permeability of the medium, $\partial(\Delta P)/\partial x$ is the pressure gradient (negative value), A is the cross-sectional area perpendicular to x, and the pressure difference $\Delta P = \Delta G/(xA) = \Delta G/V = E - W$,where ΔG is the fluid potential. Thus (Appendix subsection E)

$$\frac{\partial n}{\partial t} = \frac{k\gamma[(2R + \zeta)\cos\theta - 3R]}{\eta R^2}\frac{\partial^2 n}{\partial x^2}. \tag{7}$$

This equation has the similar solution as that of Cahn's equation [12], thus the fluctuation of cluster concentration due to inhomogeneous distribution can be represented as (Appendix subsection E)

$$n - n_c = c n_c \exp[q(\alpha)\tau]\sin(\alpha x + \phi), \tag{8}$$

where n_c is the number of homogenously distributed clusters in unit volume, τ is the time of the fluctuation, c is the decimal coefficient determined by the initial and boundary conditions, α is the wave number, q is the amplification factor,

$$q(\alpha) = k\gamma\alpha^2[3R - (2R + \zeta)\cos\theta]/\eta R^2. \tag{9}$$

Therefore, the number of clusters in the unit volume varies in spatial space by sine function. As the evaporation proceeds, ζ is continually decreasing until it satisfies $W - E \leqslant 0$, i.e., $3R - (2R + \zeta)\cos\theta \geqslant 0$. This leads to $q \geqslant 0$, i.e., the fluctuation of cluster number amplifies with time. Thus the cluster suspension is unstable and subjected to the separation

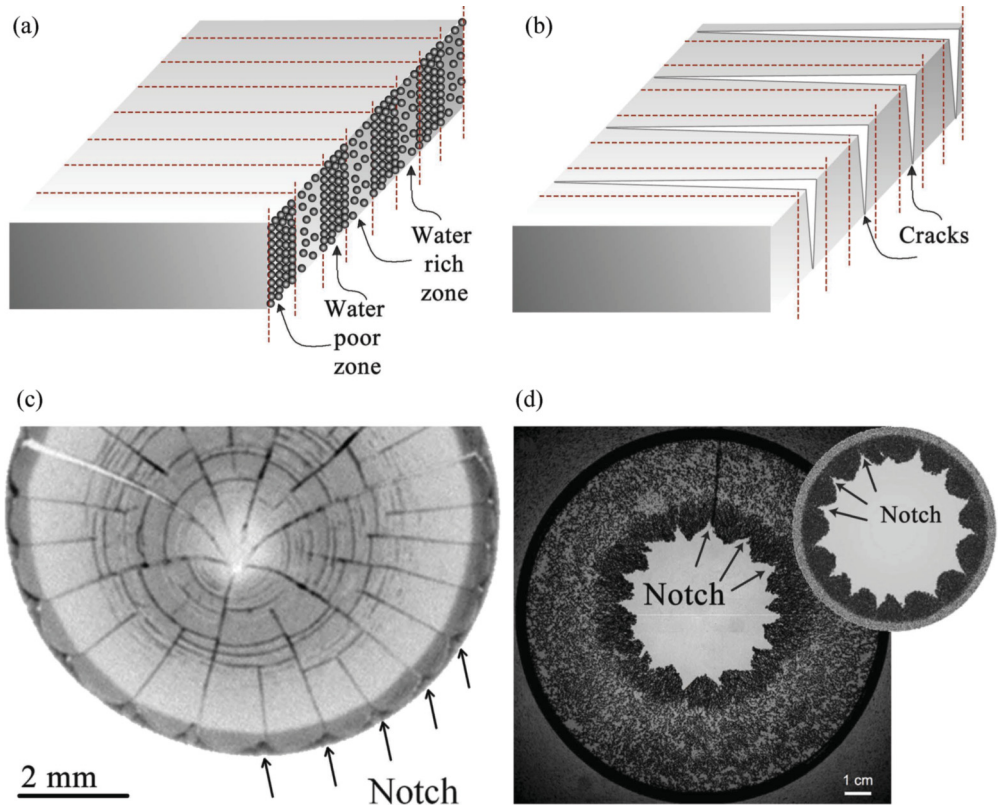

FIG. 3. (Color online) (a) Fluctuation of the number concentration of clusters. (b) Cracks nucleating at the dried sites which originally are water zones due to the phase separation. (c) Crack initiation from the periodical distribution of notches resulting from the phase separation. Drying conditions: silica aqueous suspension (particle diameter: 80 nm) from Klebosol (AZ Electronic Materials) was used as received. A drop of suspension (silica volume fraction: 27.5%) dried on glass substrate in condition: temperature: 31 °C; relative humidity: 38.5 RH%. (d) The experiment and simulation show that crack pattern results from periodical notches in the monolayer of particles at air-water interface. The periodical notches are observable using microscopic particles (diameter ~50 μm). Upper right inset: the simulation result [25].

from water similar to the spinodal decomposition [12]. As $q = 0$, the phase separation starts with the critical wave number α. The critical wave number (at $q = 0$) is (Appendix subsection F)

$$\alpha = \frac{2\pi}{\lambda} = \frac{\pi \cos\theta}{4cN_c R}, \tag{10}$$

where N_c is the cluster number at $\tau = 0$.

Equation (9) indicates that amplification factor q increases as ζ decreases, and this reduction of ζ results directly from the evaporation. In fact, as the air invades the space between the clusters, the drying process nearly completes, and the time for further evaporation is short during the phase separation. Therefore, we approximately consider ζ (or q) as the constant, and use the critical wave number (at $q = 0$) to describe the fluctuation process induced by the energy criterion $W - E \leqslant 0$.

From Eq. (10), the fluctuation wavelength is

$$\lambda = 8cN_c R/\cos\theta. \tag{11}$$

When the drying has completed, the film of dried deposition consisting of N_c clusters lies on the solid substrate of the area L. Since the substrate area L is a constant for the drying experiment, the cluster number N_c increases with film thickness H increasing. Incorporating the factor of particle size, thus, $H \propto N_c R$. Then Eq. (11) results in the relation

$$\lambda \propto H. \tag{12}$$

As the fluctuation of the cluster number proceeds during the phase separating of water and clusters, the periodical distribution of clusters forms [the cluster rich and water rich zones shown in Fig. 3(a)]. The water zone finally dries out, resulting in the periodical distribution of crevices. As know, the crack pattern induced by the embedded flaws in thin film has been theoretically analyzed [19–21] and experimentally found [22–24]. In the present study, those crevices are the kind of periodical flaws which act as the sites where periodically parallel cracks nucleate resulting from the stress in the deposition film [Fig. 3(b)]. Our experimental result clearly displays that the crack pattern was produced from the periodically distributed notches (flaws) formed by the phase separation of clusters and water [Fig. 3(c)]. The positions of notches correspond to the dried water rich zones, displaying a wavelength.

Recently, Bandi *et al.* have also discovered that the crack pattern results from periodical notches in the monolayer of hydrophobic particles at the air-water interface [Fig. 3(d)] [25]. They dipped the surfactant (oleic acid) onto this interface with Teflon-coated glass particles floating. The surfactant spread on the interface, and pushed the particles outward along the radial direction. Finally, notches formed on the ring resulting from particles packing.

It is generally considered that surfactant spreading on the air-water interface is driven by Marangoni stresses resulting from surfactant concentration gradient (along the spreading direction). Surfactant concentration fluctuation in the spreading front leads to the formation of the ramified fingers periodically lying with a specific wavelength [26,27]. This spreading front (fingers) can compress loose particles into the packing with the wavelike front [28], which resembles the periodical notches, suggesting the formation mechanism of the notch shape. Although the experimental systems are different, Bandi *et al.*'s results are helpful for understanding the physical mechanism of the present work. In summary, the cracks in the pattern initiate at the periodical flaws resulting from the phase separation of colloidal clusters and water, then prorogate under the law of fracture mechanics.

At a fixed time, the fluctuation of cluster number can be represented as a sine function [Fig. 4(a)]. The wavelength of the fluctuation is designed for the crack space (the distance between two adjacent cracks) in the dried film. In terms of the relation (12), the crack space linearly increases with film thickness increasing [Fig. 4(b)]. This theoretical predication is consistent with the well accepted experimental results [7,10].

Combining Eqs. (1), (2), and (11), thus

$$\lambda \propto N_0 r_0 \quad \text{or} \quad n_0 V_0 r_0. \tag{13}$$

This formula indicates that the crack space increases with the increment of the initial number and size of colloidal particles [Fig. 4(c)]. This prediction is also consistent with the experimental fact that as the particle size and suspension volume are constant, the crack spacing and thickness of deposition film linearly grow with the increase of initial particle concentration n_0 [4,11].

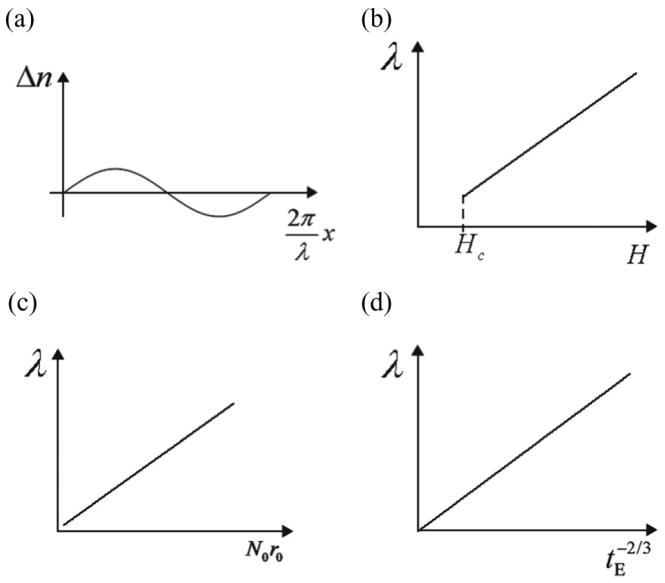

FIG. 4. Relationship between the parameters in the theory (presenting in dimensionless quantities). Fluctuation of the number of clusters displays the sine function (set initial phase ϕ as zero) (a). Crack space linearly grows with the increase of film thickness ($> H_c$, critical film thickness) (b), $N_0 r_0$ (c), and $t_E^{-2/3}$ (d), respectively.

Cracks are only produced in the deposition film whose thickness exceeds a critical value in terms of fracture mechanics [29]. There may be another reason for the production of the crack-free thin film. From the formula (12), as H is very small, so does λ. Thus the fluctuation needs too high energy to occur [30], i.e., no crack (flaw) patterns produce. This may provide the explanation for the following experimental phenomenon of dried deposition film [31]: (1) Due to the lack of flaws where cracks originated, the film was crack free when its thickness was below the critical film thickness. (2) With film thickness just reaching critical film thickness, some random cracks appeared by the principle of fracture mechanics, but no crack pattern produced since the corresponding λ was still too small to develop. (3) As film thickness continuously increased, a regular crack pattern formed since suitable λ could develop for the fluctuation.

The whole process of drying colloidal suspension can be classified into two stages. The first one is the evaporation stage, whose time is denoted as the evaporation time t_E. t_E is the time from evaporation beginning to air-liquid interface reaching the top points of clusters (e.g., O_1, O_2 in Fig. 2). Subsequently, in the second stage, the air-liquid interface invades the clusters and forms the meniscus. The further meniscus proceeding forward leads to the phase separation of the solvent and clusters. This is the stage of solvent drainage (or phase separation), lasting for the time t_d. In the experiment of drying colloidal suspension, the drainage time t_d is far less than the evaporation time t_E, i.e., $t_d \ll t_E$. t_E can be represented as (Appendix subsection G)

$$\lambda \propto t_E^{-2/3}. \tag{14}$$

Thus the fluctuation wavelength inversely changes with the evaporation time [Fig. 4(d)]. For long time evaporation, i.e., the large t_E, λ is too small to form the fluctuation. Therefore, no periodical flaws produce for inducing the cracks. This agrees with the experimental fact that crack-free thin film can be achieved by the slow drying [29].

Therefore, the sequences of crack pattern formation are as follows: First, the colloidal suspension is drying, and the colloidal clusters continually coalesce in this process. Second, in the late stage of drying, air-liquid interface reaches just above the deposition, water drainage from the clusters results in the phase separation of the clusters and water. The water zones become the periodically distributed flaws after the water has dried out. Cracks then originate from the sites of flaws in terms of fracture mechanics. Finally, the cracks develop and propagate in the deposition under the law of fracture mechanics.

In summary, we propose the theory for the origin of crack pattern in the deposition film produced by drying colloidal suspension. Before developing and propagating in the deposition under the law of fracture mechanics, the cracks initiate from the periodically distributed flaws with stress acting, making up the regular crack pattern. Those flaws result from the phase separation of the colloidal clusters and water. This phase separation is characterized by the fluctuation of cluster number with the wavelength corresponding to the crack spacing. The crack spacing linearly grows with the increasing of film thickness and initial particle concentration, which is consistent with the experimental results.

ACKNOWLEDGMENTS

The authors gratefully acknowledge the support by NSFC (Grant No. 11104218), Natural Science Basic Research Plan in Shaanxi Province of China (Program No. 2010JZ001), and Scientific Research Foundation for the Returned Overseas Chinese Scholars (Shaanxi Administration of Foreign Expert Affairs, 2011).

APPENDIX

(A) The DLVO theory is adopted to describe the interaction energy between two colloidal particles (clusters),

$$\phi = \left(\frac{2k_BT}{e}\ln\zeta + \psi_0\right) - \frac{AR}{12\zeta}. \tag{A1}$$

k_B is Boltzmann's constant, T is the temperature (K), e is the electron unit charge, ζ is the surface distance of two particles (clusters), ψ_0 is the reference potential, A is the Hamaker constant, R is the particle (cluster) radius. The first term represents the electric potential derived from the Poisson-Boltzmann equation on the condition of weak electrolyte (no added electrolyte) [32], and the second term is the van der Waals energy [33].

(B) In Fig. 5(a), consider particles diffusing across the section area s [take unit length along x (Fig. 5(b)], then the diffusion amount $Q_D = \int Jsdt$. The diffusion flux $J = D(n/y) = Dn\tan\theta_s/s = Dns_0/y_0s$, where n is the particle number concentration, y is the distance between the contact line and the reference position, y_0 is the initial distance, s is the height of the suspension at the reference position, s_0 is the initial height, θ_s is the contact angle of the suspension on substrate. The diffusion constant D is given by the Stokes-Einstein equation, $D = k_BT/6\pi\eta R$ (η, viscosity). Consequently, $Q_D = Dns_0t_0/y_0$, where t_0 is the evaporation time. The solute amount in the volume $y_0s_0/2$ [take unit length along x, Fig. 5(b)] is $M = ny_0s_0/2$.

Q_D/M ($=2Dt_0/y_0^2$) can be estimated by our experimental data, drying the drop of silica aqueous suspension on glass substrate under ambient conditions: particle diameter: 80 nm; volume fraction: 27.5%; evaporation time: 80 s; $y_0 = 340\ \mu$m. Get $Q_D/M = 0.7\%$. Thus $Q_D \ll M$, the diffusion from the right side of reference position to its left (the reaction area with the volume $y_0s_0/2$) can be neglected.

(C) We study the strip area near the contact line with the width δ [Fig. 5(b)]. Since δ is short, the difference of suspension height along the y direction can be ignored (see the section figure along XY in the inset). The suspension volume can be represented as $V = \int dV$, the variable of integration $dV = (2R+\zeta)^3$ [see Fig. 6(a); since dV is very small, particles are approximately treated as locating on the lattice sites]. For homogenously distributed particles with the number of N during the kth coalescence process,

$$V = S\left(h_0 - h_t't^e_{k-1}\right) = N(2R+\zeta)^3/4, \tag{A2}$$

where S is the evaporation area, t^e_{k-1} is the evaporation (reaction) time for completing $k-1$ coalescences ($k-1$ doublet reactions). h_0 is the initial suspension height at $t^e = 0$, h_t' ($\approx 0.1\ \mu$m/s [7]) is the evaporation rate along the height direction. Substitute Eq. (1) into (A2), get the cluster distance in the process of the kth coalescence,

$$2R+\zeta = \left[\left(\frac{2^{k+2}}{n_0}\right)\left(1 - \frac{h_t'}{h_0}t^e_{k-1}\right)\right]^{1/3}, \tag{A3}$$

where $n_0 = N_0/Sh_0 = N_0/V_0$ is the initial particle number concentration.

During the period for one coalescence, the concentration increment resulting from the evaporation is $\Delta C_E = \frac{n_0S\Delta h}{S(h_0-\Delta h)} = n_0\frac{\Delta h}{h_0}/(1-\frac{\Delta h}{h_0}) \approx n_0\frac{\Delta h}{h_0}(1+\frac{\Delta h}{h_0}) \approx n_0\Delta h/h_0, \Delta h \ll h_0$, where Δh is the height reduction resulting from the evaporation. As $\Delta h = h_t't_k$ (t_k is the time for completing one coalescence), we have

$$\Delta C_E = n_0h_t't_k/h_0 = n_0t_k/t, \tag{A4}$$

where t is the total evaporation time. For one coalescence, the number concentration halves in terms of Eq. (1). The corresponding concentration reduction (represented by negative sign) is $\Delta C_C = -C/2$, where C is the suspension concentration. For the typical cluster sizes of 10 μm and the experimental data in subsection B, times (numbers) of coalescence are given by Eq. (2), $k = 21$. The average evaporation time for one coalescence, $\langle t_k\rangle = t/k = 80\,\text{s}/21 = 3.8\,\text{s}$. From Eq. (A4), $\Delta C_E = 4.8\%\ n_0 \ll |\Delta C_C| = 50\%n_0$. Thus in the period of one coalescence, the number concentration is controlled by cluster coalescence rather than the evaporation effect, but the evaporation affects the concentration after relative long time by shortening the distance of clusters ζ, as indicated by Eq. (A3).

(D) The work is needed to be done for the drainage of water (from X to Y in Fig. 2) is $w_1 = \int_R^{-R} Fd(-z) = -\int_R^0 4\frac{2\pi r\gamma}{4}\cos(\varphi+\theta)dz - \int_0^{-R} 4\frac{2\pi r\gamma}{4}\cos(\varphi-\theta)dz$, where F is the capillary force along the z direction, θ is the contact angle of water on the spherical cluster, φ is the angle between the perpendicular and tangent lines at the contact point of the cluster with water (Fig. 2), r is the projection radius of the retreating contact line [Figs. 6(b) and 6(c)], $z = \sqrt{R^2-r^2}$ [Fig. 6(c)]. Performing the integration to get

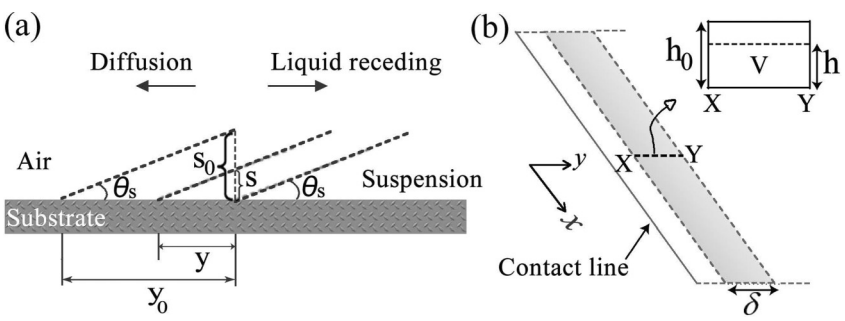

FIG. 5. (a) Sketch of suspension receding in drying process. (b) Strip area with the width δ close to the contact line. Inset: cross section of the strip area (section line XY).

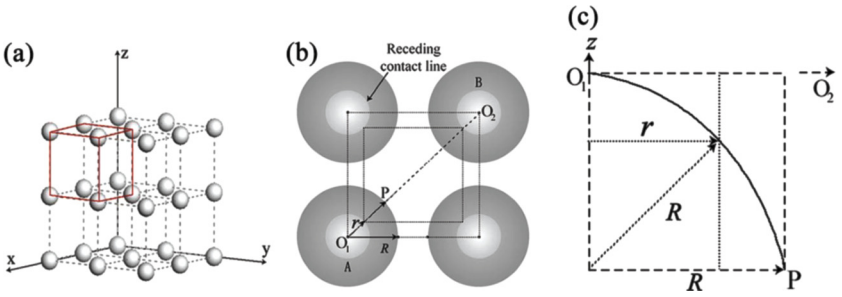

FIG. 6. (Color online) (a) Cubic representation of clusters locating at lattice sites. (b) Top view of the drainage. Small bright circle is the projection of bare spherical cap produced by the drainage. (c) Section figure along O_1P in (b).

$w_1 = \frac{8}{3}\pi\gamma R^2\cos\theta$. The extra work needed to be done for the drainage of the water between ζ (Fig. 2) is $w_2 = \bar{F}\zeta = \frac{4}{3}\pi\gamma R\zeta\cos\theta$, where $\bar{F}$ is the average force $(w_1/2R)$ during the drainage. The water drainage driven by the work $w_1 + w_2$ results in simultaneously releasing the surface energy of one cluster, $4 \times \frac{1}{4}\pi R^2\gamma$ [water drainage of the square zone in Fig. 6(b)]. Thus the total work for water drainage in unit volume is

$$W = n(w_1 + w_2) = \tfrac{4}{3}\pi\gamma nR(2R+\zeta)\cos\theta.$$

(E) The pressure driving the water flowing through the porous medium (clusters) is

$$\begin{aligned}\Delta P &= \Delta G/(xA)\\ &= E - W = 4\pi\gamma nR\big(R - \tfrac{1}{3}(2R+\zeta)\cos\theta\big).\end{aligned} \tag{A5}$$

The flow rate can also be represented as

$$Q = \frac{\partial V_w}{\partial t} = \frac{\partial(1-4\pi R^3 n/3)V_s}{\partial t} = -\frac{4\pi R^3 V_s}{3}\frac{\partial n}{\partial t}, \tag{A6}$$

where V_w is the change of water volume due to the drainage of suspension volume V_s. Take the derivative of Eqs. (6) and (A6) with x and combine with $\partial V_s/\partial x = A$ and Eq. (A5), we get

$$\frac{\partial n}{\partial t} = \frac{k\gamma[(2R+\zeta)\cos\theta - 3R]}{\eta R^2}\frac{\partial^2 n}{\partial x^2}.$$

This equation has the similar solution as that of Cahn's equation [12], which represents Fourier components of the fluctuation of cluster concentration due to inhomogeneous distribution,

$$n - n_c = \sum_{\alpha_i}\exp[q(\alpha_i)\tau][B(\alpha_i)\cos\alpha_i x + K(\alpha_i)\sin\alpha_i x], \tag{A7}$$

where n_c is the number of homogenously distributed clusters in unit volume, τ is the time of the fluctuation, α_i is the wave number. B and K are coefficients evaluated at $\tau = 0$ by the boundary conditions. q is the amplification factor. In the present study, as $q = 0$, the phase separation starts with the critical wave number α. Thus, Eq. (A7) can be written as

$$n - n_c = \exp[q(\alpha)\tau][B(\alpha)\cos\alpha x + K(\alpha)\sin\alpha x].$$

Thus,

$$\begin{aligned}n - n_c = {}&\sqrt{B^2+K^2}\exp[q(\alpha)\tau]\\ &\times\left(\frac{B}{\sqrt{B^2+K^2}}\cos\alpha x + \frac{K}{\sqrt{B^2+K^2}}\sin\alpha x\right),\end{aligned} \tag{A8}$$

where $\sqrt{B^2+K^2} = cn_c$, c is the decimal coefficient determined by the initial and boundary conditions. Make $\frac{K}{\sqrt{B^2+K^2}} = \cos\phi$, $\frac{B}{\sqrt{B^2+K^2}} = \sin\phi$, write Eq. (A8) as

$$n - n_c = cn_c\exp[q(\alpha)\tau]\sin(\alpha x + \phi).$$

(F) Take the derivative of two sides of Eq. (A2), we have

$$(2R+\zeta)\frac{dN}{dx} + 3N\frac{d\zeta}{dx} = 0. \tag{A9}$$

The coordination x can be represented as $x = N(2R+\zeta)$. Take its derivative,

$$N\frac{d\zeta}{dx} = 1 - (2R+\zeta)\frac{dN}{dx}. \tag{A10}$$

Substitute (A10) into (A9) to get

$$(2R+\zeta)\frac{dN}{dx} = \frac{3}{2}. \tag{A11}$$

To evaluate dN/dx, multiply V and take the derivative of two sides of Eq. (8) at $\tau = 0$; it gives

$$dN/dx = \alpha cN_c\cos(\alpha x + \phi). \tag{A12}$$

Substitute Eq. (A12) into Eq. (A11) to get

$$(2R+\zeta)\cos(\alpha x + \phi) = \frac{3}{2c\alpha N_c}. \tag{A13}$$

To evaluate $2R+\zeta$, make $\beta = \alpha x + \phi$ and integrate equation (A13) with β in the interval $[-\pi/2, \pi/2]$, that is, $2R+\zeta = \frac{3\pi}{4c\alpha N_c}$. Substitute it into Eq. (9), we get

$$q = \frac{3k\gamma\alpha^2}{\eta R^2}\left(R - \frac{\pi\cos\theta}{4c\alpha N_c}\right).$$

The critical wave number α corresponds to $q = 0$, thus,

$$\alpha = \frac{2\pi}{\lambda} = \frac{\pi\cos\theta}{4cN_cR}.$$

(G) In the RLCA process, a number of collisions lead to one coalescence. The coalescence probability of particle collision is P = number of coalescence/number of collision [34]. The characteristic time for doublet formation has been derived from the probability density theory [35]. Combining P into this result, we get the time for completing one coalescence,

$$t_k = \frac{\pi\eta W R^3}{k_B T P\nu}, \tag{A14}$$

where the stability ratio $W = \frac{2R}{r_m^2}\left(\frac{2\pi k_B T}{-(\partial^2\phi/\partial r^2)_{r_m}}\right)^{1/2}e^{\phi_m/k_BT}$, ϕ_m is the maximum potential evaluated by the derivative of Eq. (A1), satisfying $(d\phi/dr)_{r_m} = 0$, $r_m(=2R+\zeta_m)$ is the distance between the centers of two adjacent clusters (as $\phi = \phi_m$), $(\partial^2\phi/\partial r^2)_{r_m}$ (negative value) is the second derivative of ϕ at r_m. The cluster volume fraction

$\nu = N\frac{4}{3}\pi R^3/\frac{N}{4}(2R+\zeta)^3 = \frac{16\pi}{3}(\frac{R}{2R+\zeta})^3$, thus

$$t_k = \frac{3\eta W(2R+\zeta)^3}{16k_BTP}. \tag{A15}$$

Combining Eqs. (A3) and (A15), the total time for finishing k times (numbers) of coalescences is

$$t = \sum_{k=1}^{k} t_k = \frac{3\eta W}{16k_BTPn_0}\sum_{k=1}^{k} 2^{k+2}\left(1 - \frac{h_t'}{h_0}t_{k-1}^e\right). \tag{A16}$$

As the kth coalescence proceeding, the evaporation time having been experienced (since $t^e = 0$) is the sum of the time for $k-1$ times of coalescences,

$$t_{k-1}^e = \sum_{k=1}^{k-1} t_k. \tag{A17}$$

Substitute Eq. (A17) into Eq. (A16), perform series expansion and make approximation, we reach an equation

$$t \approx \frac{2^k 3\eta W}{2k_BTPn_0}\left(1 - \frac{h_t'}{h_0}t\right). \tag{A18}$$

Solving the equation, we get the times (numbers) of coalescences before the phase separation of water and clusters,

$$k = \log_2 \frac{2k_BTPn_0h_0t}{3\eta W(h_0 - h_t't)}. \tag{A19}$$

Combining Eqs. (1), (2), (11), and (A19) results in the relation

$$\lambda \propto \left(\frac{3\eta W(h_0 - h_t't)}{2k_BTPn_0h_0t}\right)^{2/3}. \tag{A20}$$

Define the constant $I = (\frac{3\eta W}{2k_BTPn_0})^{2/3}$, $t = t_E$ as the evaporation time before the water drainage occurs, and impose the conditions $\frac{h_t'}{h_0}t_E < 1$, $\frac{2}{3}\frac{h_t'}{h_0} \ll 1$, the formula (A20) can be written as $\lambda \propto t_E^{-2/3}I(1 - \frac{h_t'}{h_0}t_E)^{2/3} \approx t_E^{-2/3}I(1 - \frac{2}{3}\frac{h_t'}{h_0}t_E) \sim t_E^{-2/3}I$. Consequently,

$$\lambda \propto t_E^{-2/3}.$$

[1] L. Goehring and S. W. Morris, Europhys. Lett. **69**, 739 (2005).
[2] K. A. Shorlin, J. R. de Bruyn, M. Graham, and S. W. Morris, Phys. Rev. E **61**, 6950 (2000).
[3] T. Okubo, M. Nozawa, and A. Tsuchida, Colloid Polym. Sci. **285**, 827 (2007).
[4] T. Okubo, K. Kimura, and H. Kimura, Colloid Polym. Sci. **280**, 1001 (2002).
[5] T. Mizuguchi, A. Nishimoto, S. Kitsunezaki, Y. Yamazaki, and I. Aoki, Phys. Rev. E **71**, 056122 (2005).
[6] E. Dufresne, D. Stark, N. Greenblatt, J. Cheng, J. Hutchinson, L. Mahadevan, and D. Weitz, Langmuir **22**, 7144 (2006).
[7] C. Allain and L. Limat, Phys. Rev. Lett. **74**, 2981 (1995).
[8] M. S. Tirumkudulu and W. B. Russel, Langmuir **20**, 2947 (2004).
[9] G. Gauthier, V. Lazarus, and L. Pauchard, Langmuir **23**, 4715 (2007).
[10] L. Pauchard, M. Adda-Bedia, C. Allain, and Y. Couder, Phys. Rev. E **67**, 027103 (2003).
[11] T. Okubo, T. Yamada, K. Kimura, and A. Tsuchida, Colloid Polym. Sci. **283**, 1007 (2005).
[12] J. W. Cahn, J. Chem. Phys. **42**, 93 (1965).
[13] M. Hütter, Ph.D. thesis, Swiss Federal Institute of Technology, Zurich, 1999.
[14] P. C. Hiemenz and R. Rajagopalan, *Principles of Colloid and Surface Chemistry* (Marcel Dekker, New York, 1997).
[15] S. V. Roth, A. Rothkirch, T. Autenrieth, R. Gehrke, T. Wroblewski, M. C. Burghammer, C. Riekel, L. Schulz, R. Hengstler, and P. Müller-Buschbaum, Langmuir **26**, 1496 (2009).
[16] J. Groenewold and W. Kegel, J. Phys.: Condens. Matter **16**, S4877 (2004).
[17] S. V. Roth, P. Muller-Buschbaum, A. Timmann, J. Perlich, and R. Gehrke, Appl. Crystallography **40**, s346 (2007).
[18] C. W. Fetter, *Applied Hydrogeology*, 4th ed. (Prentice-Hall, Englewood Cliffs, NJ, 2000).
[19] Z. C. Xia and J. W. Hutchinson, J. Mech. Phys. Solids **48**, 1107 (2000).
[20] W. B. Russel, N. Wu, and W. Man, Langmuir **24**, 1721 (2008).
[21] A. Sarkar and M. S. Tirumkudulu, Phys. Rev. E **83**, 051401 (2011).
[22] G. Jing and J. Ma, J. Phys. Chem. B **116**, 6225 (2012).
[23] W. Man and W. B. Russel, Phys. Rev. Lett. **100**, 198302 (2008).
[24] S. Nurkhamidah and E. Woo, Colloid Polym. Sci. **290**, 275 (2012).
[25] M. Bandi, T. Tallinen, and L. Mahadevan, Europhys. Lett. **96**, 36008 (2011).
[26] O. K. Matar and S. M. Troian, Phys. Fluids **10**, 1234 (1998).
[27] O. Matar and R. Craster, Soft Matter **5**, 3801 (2009).
[28] L. R. Gómez, A. M. Turner, M. van Hecke, and V. Vitelli, Phys. Rev. Lett. **108**, 58001 (2012).
[29] P. Xu, A. S. Mujumdar, and B. Yu, Drying Technol. **27**, 636 (2009).
[30] R. A. L. Jones, *Soft Condensed Matter* (Oxford University Press, Oxford, 2002).
[31] A. Atkinson and R. M. Guppy, J. Mater. Sci. **26**, 3869 (1991).
[32] D. Andelman, in *Handbook of Biological Physics: Structure and Dynamics of Membranes*, edited by R. Lipowsky and E. Sackmann, Vol. 1B (Elsevier Science B.V., Amsterdam, 1995), p. 603.
[33] J. N. Israelachvili, *Intermolecular and Surface Forces*, 2nd ed. (Academic, London, 1992).
[34] A. AlSunaidi, M. Lach-Hab, A. E. González, and E. Blaisten-Barojas, Phys. Rev. E **61**, 550 (2000).
[35] W. B. Russel, D. A. Saville, and W. R. Schowalter, *Colloidal Dispersions* (Cambridge University Press, Cambridge, England, 1989).